

# In-medium bound states and pairing gap

O.A. Rubtsova,\* V.I. Kukulin,† and V.N. Pomerantsev‡

*Skobeltsyn Institute of Nuclear Physics, Moscow State University, Leninskie gory, Moscow, 119991, Russia*

H. Mütter§

*Institute for Theoretical Physics, University of Tübingen,  
Auf der Morgenstelle 14, D-72076 Tübingen, Germany*

The propagator of two nucleons in infinite nuclear matter is evaluated by a diagonalization of the *pphh* RPA Hamiltonian. This effective Hamiltonian is non-Hermitian and, for specific density domains and partial waves, yields pairs of complex conjugated eigenvalues representing in-medium bound states of two nucleons. The occurrence of these complex poles in the two-particle Greens function is tightly related to the well known BCS pairing approach. It is demonstrated that these complex eigenvalues and the corresponding bound state wavefunctions contain all information about the BCS gap function. This is illustrated by calculations for  $^1S_0$  and  $^3PF_2$  pairing gaps in neutron matter which essentially coincide with the corresponding gap functions extracted from conventional solutions of the gap equation. Differences between the bound states in the conventional BCS approach and the *pphh* RPA are arising in the case of  $^3SD_1$  channel in symmetric nuclear matter at low densities. These differences are discussed in the context of transition from BEC for quasi-deuterons to the formation of BCS pairing.

PACS numbers: 21.65.-f, 21.60.De, 24.10.Cn

## I. INTRODUCTION

The pairing of fermions in Fermi liquids has been studied in detail many decades ago and became an important part of fundamental science and a corner stone of the theories on superfluidity and superconductivity [1, 2]. In the conventional way in BCS method [2] or Bogolyubov's approach one derives and solves the non-linear gap equation for the gap function  $\Delta(k)$  which describes the deviation of the single particle energies from continuous spectrum near the Fermi-surface. This procedure has successfully been used in solid state physics and later has been applied also for studying superfluidity in nuclear matter [3–5]. The values for the gap in the  $^1S_0$  channel for neutron matter extracted from such calculations turned out to be in a reasonable agreement with empirical data for neutron-neutron and proton-proton pairing in finite nuclei. In neutron matter at densities above the saturation density of symmetric nuclear matter the pairing of neutrons in the  $^3PF_2$  channel occurs also and may become relevant for understanding the cooling of neutron stars [6–8].

The interaction between proton and neutron in the triplet  $^3SD_1$  channel, however, is more attractive than the interaction between two neutrons in  $^1S_0$  channel and leads to the vacuum bound state of two nucleons in the deuteron channel  $^3SD_1$ . Therefore one would expect even stronger pairing effects from proton-neutron pairing

in isospin symmetric nuclear systems. Indeed, BCS calculations for symmetric nuclear matter lead to a sizable gap of around 10 MeV at the empirical saturation density [9–12]. The empirical data for finite nuclei with number of protons close to the number of neutrons, however, do not show any indications of strong proton neutron pairing, which would correspond to a pairing gap as large as 10 MeV.

Therefore attempts have been made to embed the BCS approach into more general scheme for evaluating self-consistent Greens's functions (SCGF). Usually this is done in the framework of a generalized mean field approach within the well known Nambu–Gorkov formalism with an explicit BCS parameterization for single particle energies and the respective Green's functions. More generally [13] one tries to solve SCGF equations in the  $T$ -matrix or ladder approximation with a self-consistent evaluation for single-particle and two-particle Green functions. Employing realistic models for the nucleon-nucleon (NN) interactions, i.e. NN potentials which fit the NN scattering data such as the Argonne V18 [14] or CD-Bonn potential [15], one obtains significant deviations from the mean-field results. The strong short-range and tensor components of such realistic NN interactions lead to non-negligible depletions of the occupation of states with momenta below the Fermi momentum  $k_F$  and corresponding occupations of states with momenta larger  $k_F$ .

The central equation to be solved with such SCGF calculations is scattering or  $T$ -matrix equations for a pair of interacting nucleons in nuclear matter. The resulting  $T$ -matrix is used to define the nucleon self-energy, which is needed to evaluate the single-particle (sp) Green's function. Since the information on energy- and momentum-distribution of the single-particle strength, which is con-

---

\*Electronic address: rubtsova@nucl-th.sinp.msu.ru

†Electronic address: kukulin@nucl-th.sinp.msu.ru

‡Electronic address: pomeran@nucl-th.sinp.msu.ru

§Electronic address: herbert.muether@uni-tuebingen.de

tained in the *sp* Green's function, is required to set up *T*-matrix equation, the evaluation of the *sp* Green's function and the solution of the corresponding *T*-matrix equation have to be done in a self-consistent manner. The solution of the *T*-matrix integral equation is complicated due to the so-called pairing instabilities which are related to the occurrence of quasi-bound two-nucleon states in the nuclear medium [16].

On the other hand, we have recently developed a formalism in which the two-particle Green's function is evaluated in terms of discrete eigenvalues and eigenfunctions of a two-particle Hamiltonian [17]. This approach allows to treat two-particle continuum and two-particle bound states in vacuum and also in medium on the same footing. It has been applied to evaluate the NN scattering phase-shifts as well as the solution of Bethe–Goldstone equation, the nuclear *G*-matrix, in an efficient way. In the present paper we will generalize this approach to include not only the particle-particle states (*pp*), as it has been done for Bethe–Goldstone equation, but also the hole-hole states (*hh*) in evaluating the in-medium *T*-matrix. This approach leads to the diagonalisation of an effective Hamiltonian, which corresponds to the *pphh* RPA Hamiltonian.

The eigenvalues of this Hamiltonian become complex in the region of pairing instabilities. This implies that the occurrence of such instabilities in the framework of the SCGF is under control. In the mean-field limit for the single-particle Green's function the RPA equation for two nucleons with c.m. momentum equal to zero correspond to the BCS approach. Here it is worth to mention the novel stabilization technique[18]. In this technique one determines the gap function at the Fermi surface from the imaginary part of the complex eigenvalues of *pphh* RPA.

In the present paper we will demonstrate that not only the complex eigenvalues of the effective Hamiltonian can be used in finding the gap in the vicinity of Fermi surface but the corresponding eigenfunctions of these eigenvalues are also directly related to the momentum dependence of the gap function for all momenta. This yields a new method for finding the gap function which is efficient in particular for pairing in coupled channels such as  ${}^3PF_2$  in the case of neutron-neutron pairing or  ${}^3SD_1$  for proton-neutron pairing.

For the sake of simplicity we restrict our study in the present work to the case of zero temperature and use the independent particle limit for the single-particle Green's function. The present approach can be also extended to non-zero temperature and employment of dressed single-particle Green's function in the SCGF approach [19].

In the next section we will show how the complex eigenvalues and eigenfunctions of the *pphh* RPA equation are related to the gap function derived from the BCS approach. Applications for this new method to solve the BCS equation in the case of neutron matter will be discussed in section III and section IV shows results for proton-neutron pairing in the quasi-deuteron channel of

symmetric nuclear matter. Conclusions are presented in the final section V.

## II. EFFECTIVE TWO-BODY HAMILTONIAN.

### A. Equation for the *T*-matrix

Consider the equation for the in-medium *T*-matrix in which hole-hole (*hh*) degrees of freedom are also included:

$$T(E) = V + VG_{II}^0(E)T(E), \quad (1)$$

where *V* is a bare interaction and  $G_{II}^0$  is the non-interacting two-body *pphh*-propagator

$$G_{II}^0(E) = \int d\mathbf{k}_1 d\mathbf{k}_2 |\mathbf{k}_1, \mathbf{k}_2\rangle G_{II}^0(k_1, k_2; E) \langle \mathbf{k}_1, \mathbf{k}_2|. \quad (2)$$

If we consider the mean-field approximation the kernel takes the form [13]:

$$G_{II}^0(k_1, k_2; E) = \frac{\theta(k_1 - k_F)\theta(k_2 - k_F)}{E + i0 - (e_{k_1} + e_{k_2})} - \frac{\theta(k_F - k_1)\theta(k_F - k_2)}{E - i0 - (e_{k_1} + e_{k_2})}. \quad (3)$$

Here  $k_1$  and  $k_2$  are single particle momenta,  $e_k$  are single particle energies,  $k_F$  is the Fermi-momentum and all the states are antisymmetrized.

The operator  $G_{II}^0$  can formally be written as a generalized resolvent for the free Hamiltonian which includes both *pp*- and *hh*- continuum contributions:

$$H_0 = \int_{k_1, k_2 \leq k_F} d\mathbf{k}_1 d\mathbf{k}_2 |\mathbf{k}_1, \mathbf{k}_2\rangle [e_{k_1} + e_{k_2}] \langle \mathbf{k}_1, \mathbf{k}_2| + \int_{k_1, k_2 > k_F} d\mathbf{k}_1 d\mathbf{k}_2 |\mathbf{k}_1, \mathbf{k}_2\rangle [e_{k_1} + e_{k_2}] \langle \mathbf{k}_1, \mathbf{k}_2|. \quad (4)$$

So that, one can express the *pphh*-propagator through  $H_0$  Hamiltonian:

$$G_{II}^0(E) = [EJ + i0 - JH_0]^{-1}, \quad (5)$$

where *J* is the operator with the following representation in momentum space:

$$J(k_1, k_2) = \theta(k_1 - k_F)\theta(k_2 - k_F) - \theta(k_F - k_1)\theta(k_F - k_2), \quad (6)$$

Further, the two-body *T*-matrix (1) can be rewritten in a form

$$T(E) = V + VG_{II}(E)V, \quad (7)$$

where we introduced the operator  $G_{II}$  which should satisfy the integral equation:

$$G_{II} = G_{II}^0 + G_{II}^0 V G_{II} = [G_{II}^0(E)^{-1} - V]^{-1}. \quad (8)$$

By using the expression (5) one gets the following form of the above operator:

$$G_{II}(E) = [EJ + i0 - JH]^{-1}, \quad (9)$$

where

$$H = H_0 + JV. \quad (10)$$

By comparing eqs. (5) and (9) one concludes that the Hamiltonian  $H$  can be considered as an effective two-body Hamiltonian describing interaction of particles and holes. This effective Hamiltonian corresponds to the Hamiltonian of the *pphh* RPA.

The accurate formalism for a practical treatment of this type operator and the evaluation of the  $T$ -matrix will be published elsewhere [19]. In the present paper, we focus on the study of the bound states of this effective Hamiltonian in a case of zero center of mass momentum  $K = 0$  and concentrate on the occurrence of pairing phenomena.

### B. In-medium bound states and the gap equation

Because the total Hamiltonian (10) is non-Hermitian but real it may have pairs of complex conjugated eigenfunctions  $|\psi\rangle$  and  $|\psi^*\rangle$  and respective complex conjugated eigenenergies  $E_b$  and  $E_b^*$ .

We emphasize that the bound state  $|\psi\rangle$  of  $H$  is at the same time the eigenfunction of the homogeneous equation corresponding to eq. (1), i.e.:

$$H|\psi\rangle = E_b|\psi\rangle \iff G_{II}^0(E_b)V|\psi\rangle = \eta(E_b)|\psi\rangle, \quad (11)$$

with unit eigenvalue  $\eta(E_b) = 1$ . The latter equation has been studied in the stabilization approach [8, 18], where the positions of the eigenvalues  $E_b = E_0 + i\Gamma_0$  in a complex energy plane have been examined. The above approach uses the fact that the real part of the eigenvalue  $E_0 \approx 2e_F$  (where  $e_F$  is the Fermi-energy) while the imaginary part  $\Gamma_0$  coincides with the pairing gap  $\Delta(k_F)$  at the Fermi-momentum.

We will demonstrate below that the bound state wave functions are also important objects as they are related directly to the momentum dependence of the pairing gap  $\Delta(k)$ . The Schroedinger equation on the left from arrow in eq. (11) is reduced to the following system in the representation of the relative momentum  $k$ :

$$J_k(2e_k - E_0 - i\Gamma_0)\psi(k) = - \int dk' k'^2 V(k, k')\psi(k'), \quad (12)$$

where factor  $J_k = \theta(k - k_F) - \theta(k_F - k)$  is equal to 1 or  $-1$  for *pp* and *hh* parts of the continuum respectively and the integral is taken over all intermediate momentum states. The solution of the eq. (12) can be rewritten in a form:

$$\psi(k) = \frac{f(k)}{J_k(2e_k - E_0 - i\Gamma_0)}. \quad (13)$$

The equation (12) has a similar form to the equation for the gap wave function (or anomalous density)  $\chi(k)$  in the BCS approach:

$$\chi(k)2E_k = - \int dk' k'^2 V(k, k')\chi(k'), \quad (14)$$

$$\chi(k) = \frac{\Delta(k)}{2E_k}, \quad E_k = \sqrt{(e_k - e_F)^2 + \Delta^2(k)}$$

where  $\Delta(k)$  is the gap function.

We note the interesting fact (which can be easily proven for a case when the bare interaction is given by a separable potential  $V = \lambda|\varphi\rangle\langle\varphi|$ ) that solutions of the eqs. (12) and (14) are interrelated to each other up to energy terms, so that one has an approximate formula:

$$|f(k)| \approx A|\Delta(k)|, \quad (15)$$

where  $A$  is some normalization constant. Here we use absolute value of function because  $f(k)$  is complex.

For the case of a realistic bare interaction  $V$  we found that the relation (15) is valid in a very good approximation. It is likely correct to the extent that one uses the approximation of the fixed gap in the left hand side of the eq. (14), i.e.  $E_k = \sqrt{(e_k - e_F)^2 + \Delta^2(k_F)}$ .

On the basis of the eq. (15), we may suggest that the absolute value of the bound state wave function takes the following form:

$$|\psi(k)| \approx A\phi(k), \quad (16)$$

where  $A$  is a normalization factor and  $\phi(k)$  is a characteristic function defined by:

$$\phi(k) = \frac{|\Delta(k)|}{\sqrt{(2e_k - E_0)^2 + \Gamma_0^2}}, \quad \int_0^\infty |\phi(k)|^2 k^2 dk = \frac{1}{A^2}. \quad (17)$$

Below we will check this relation numerically and will use it to determine the gap functions in neutron and symmetric nuclear matter.

## III. NEUTRON MATTER CASE

For practical calculations we have used the discrete stationary wave-packet basis (SWP) [17] which corresponds to a discretization of the relative momentum  $k$ , so that, the eigenfunctions of  $H$  can be found from a diagonalisation procedure for its matrix in the SWP basis. All calculations in the following sections have been performed using the CD Bonn potential [15] and considering the kinetic energy for the single-particle energies  $e_k$ .

### A. Spin-singlet channel

In Fig. 1 comparisons of the functions  $\psi(k)$  and  $A\phi(k)$  are presented for the spin-singlet  $^1S_0$  channel in neutron

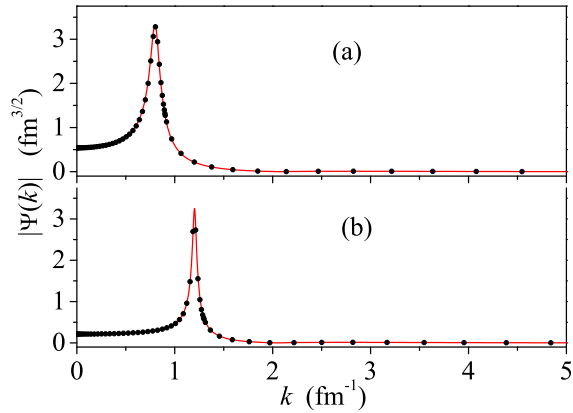


FIG. 1: (Color online) The bound-state wave function of the Hamiltonian  $H$  (solid curve) in comparison with characteristic function  $A\phi(k)$  (filled circles) at  $k_F=0.8$  (a) and  $1.2 \text{ fm}^{-1}$  (b).

matter at  $k_F=0.8$  and  $1.2 \text{ fm}^{-1}$ . Both functions are normalized to unity in momentum space. Here the function  $\phi(k)$  is defined from the pairing gap  $\Delta(k)$  calculated from solution of the BCS gap equation in a conventional way while the function  $\psi(k)$  is found from a direct diagonalisation procedure for the total Hamiltonian  $H$  matrix in the stationary wave-packet basis<sup>1</sup> [17]. It is evident from Fig. 1 that both functions are almost indistinguishable.

If one considers furthermore in dependence on the stabilization approach [8, 18] that  $\Gamma_0$  defines the pairing gap at the Fermi-momentum, it is possible to extract the momentum dependence of the gap  $\Delta(k)$  just from our bound state wave function:

$$|\Delta(k)| \approx \frac{|\psi(k)|}{|\psi(k_F)|} \sqrt{(2e_k - E_0)^2 + \Gamma_0^2}. \quad (18)$$

In Fig. 2 the gaps (the absolute values) for the  $^1S_0$  channel found from the formula (18) are presented in comparison with direct solutions of the non-linear integral gap equation for  $k_F = 0.8$  and  $1.2 \text{ fm}^{-1}$ .

The agreement is excellent. Therefore, we may conclude that the bound state wave function of the total Hamiltonian contains all the information about the pairing gap function.

### B. Spin-triplet channel

In a case of the coupled channel  $^3PF_2$ , the bound state wave function can be represented as a sum of the partial wave contributions:

$$|\psi(k)|^2 = |\psi^{l=1}(k)|^2 + |\psi^{l=3}(k)|^2. \quad (19)$$

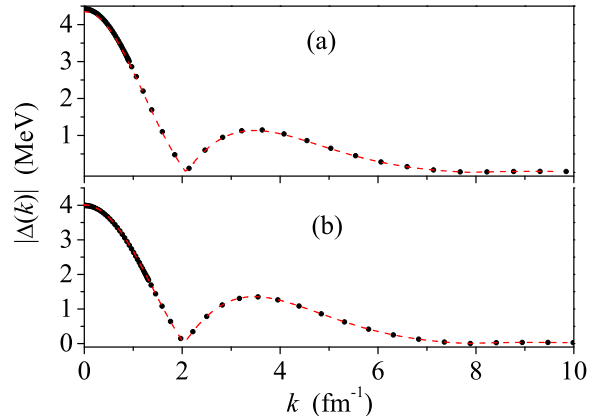


FIG. 2: (Color online) The absolute value of the gap  $\Delta(k)$  found from the bound state wave function (dashed curves) in comparison with direct solutions of the gap-equation (filled circles) for the  $^1S_0$  channel at  $k_F=0.8 \text{ fm}^{-1}$  (a) and  $1.2 \text{ fm}^{-1}$  (b).

However, the general structure is the same as in the singlet channel case, i.e.

$$|\psi(k)|^2 \approx A^2 \phi^2(k), \quad \phi^2(k) = \frac{\Delta_{l=1}^2(k) + \Delta_{l=3}^2(k)}{(2e_k - E_0)^2 + \Gamma_0^2}, \quad (20)$$

which is consistent with the relation for the two-channel total gap  $\Delta^2(k) = \Delta_{l=1}^2(k) + \Delta_{l=3}^2(k)$ .

We treat the coupled-channel case in Fig. 3 where the bound state wave functions for the  $^3PF_2$  channel are displayed in comparison with characteristic wave functions  $\phi(k)$  (normalized to unity). Here the pairing gap found from the solution of the coupled-channel gap-equation is used to find the function  $\phi(k)$ . The agreement is again perfect.

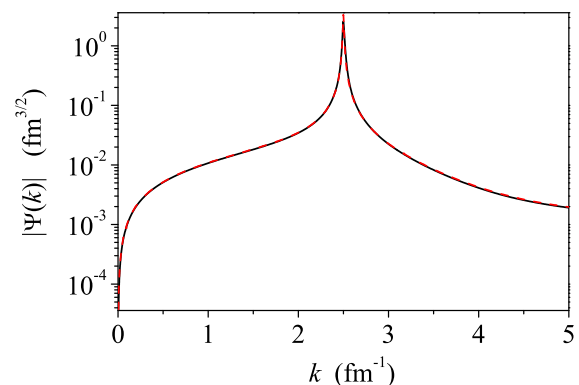


FIG. 3: (Color online) The bound-state wave function of the RPA Hamiltonian  $H$  (solid curve) in comparison with characteristic function  $A\phi(k)$  (dashed curve) for the  $^3PF_2$  channel in neutron matter at  $k_F = 2.5 \text{ fm}^{-1}$ .

<sup>1</sup> The details of the procedure will be published elsewhere [19].

A direct comparison of the gaps for  ${}^3PF_2$  channel extracted from the bound-state wave functions and those found from a direct solution of the gap integral equation is shown in Fig. 4.

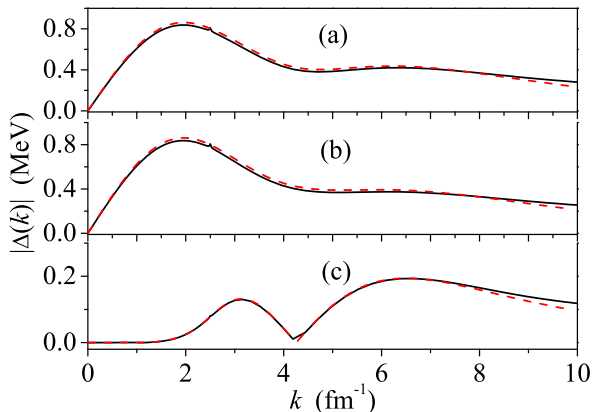


FIG. 4: (Color online) The absolute value of the gap  $\Delta(k)$  found from the bound state wave function (dashed curves) in comparison with solutions of the gap-equation (solid curves) for the  ${}^3PF_2$  channel at  $k_F = 2.5 \text{ fm}^{-1}$  (a) and the partial gaps for the partial  $P$  (b) and  $F$  (c) waves.

Thus, it appears that the eigenfunctions of the total Hamiltonian corresponding to the complex-valued bound states near the Fermi surface contain all the required information about the pairing gap. This result demonstrates clearly that a solution of the nonlinear gap equation can be replaced (at least in a case of neutron matter) with much simpler solving for the effective eigenvalue problem even in a case of coupled channels.

#### IV. THE ${}^3SD_1$ CHANNEL IN SYMMETRIC NUCLEAR MATTER

To make the picture more complete, we also consider the case of  ${}^3SD_1$  channel in symmetric nuclear matter. The main difference as compared to the cases discussed above for neutron matter is the more attractive interaction in this channel, which leads to the bound state of the deuteron in the limit of zero density.

The evolution of the bound state energy of  $H$  with increasing Fermi momentum  $k_F$  is displayed in Fig. 5. The energy scale in this figure is chosen in such a way that the continuum for two hole states is above the dotted line denoted with "threshold  $E=0$ ".

At zero  $k_F$  the Hamiltonian  $H$  has the same bound state as the the  $NN$  Hamiltonian in free space. It corresponds to the energy of the deuteron at around -2.23 MeV. With increasing  $k_F$ , the bound state energy  $E_b$  of  $H$  still remains below the  $hh$  threshold and thus is real (the blue solid curve in Fig. 5). Moreover, at some density (at  $k_F \sim 0.14 \text{ fm}^{-1}$ ), the second real bound-state

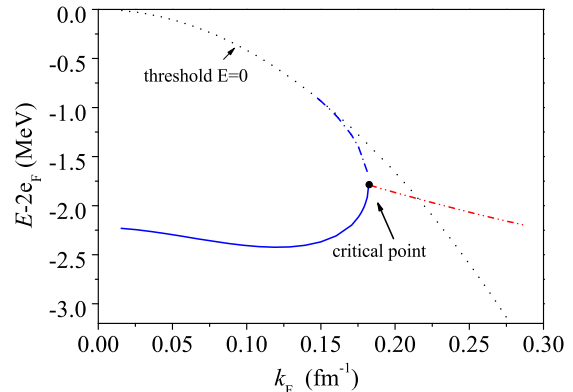


FIG. 5: (Color online) Behavior of the real-valued bound-state energies (blue curves) and the real part of the complex-valued bound-state energies (red curve) for small  $k_F$  values in the spin-triplet  $NN$  channel at  $K = 0$ .

arises under the threshold  $E = 0$  (the blue dash-dotted curve). Then, at another critical density  $k_F^C \approx 0.182 \text{ fm}^{-1}$  these two bound states merge to one point (the black filled circle) and for the higher  $k_F$  they are transformed into the pair of complex conjugated bound states  $E_b$  and  $E_b^*$  (the real part of these eigenvalues is denoted by the red dash-dot-dotted curve). Thus, at very low density our total Hamiltonian treatment leads to a picture that differs from the conventional BCS approach. The main difference is related to the fact that for Fermi momenta below a critical value  $k_F^C$  bound states occur with real energies below the threshold of the  $hh$  continuum.

This may lead to the conclusion that at densities with Fermi momenta below  $k_F^C$  the formation of bound quasi-deuterons is energetically favorable as compared to the formation of BCS Cooper pairs. At these low densities the quasi-deuterons may form a Bose-Einstein Condensate (BEC) of deuterons with zero total momentum [20, 21] and the critical Fermi momentum  $k_F^C$  would be interpreted to describe the phase transition from BEC to BCS. It should be noted, however, that our estimate for this BEC-BCS transition is not very realistic in the sense that we ignore the Coulomb interaction between protons, the contributions of electrons and the formation of isospin asymmetric nuclear matter as well as the possibility to form nuclear cluster larger than the deuteron as e.g.  $\alpha$ -cluster.

In Fig. 6 we compare the pairing gaps at  $k_F$  found from the solution of the gap equation with imaginary parts of the total Hamiltonian eigenvalues. For the region  $k_F < k_F^C$  at which  $E_b$  is real, the latter value is stated as zero. One can see from this figure that the pairing gap  $\Delta(k_F)$  derived from the imaginary part of the  $pphh$  RPA eigenstate is below the pairing gap obtained from a conventional solution of the BCS equation also at densities above  $k_F^C$ . This is probably related to the fact that also for these densities the real part of the lowest

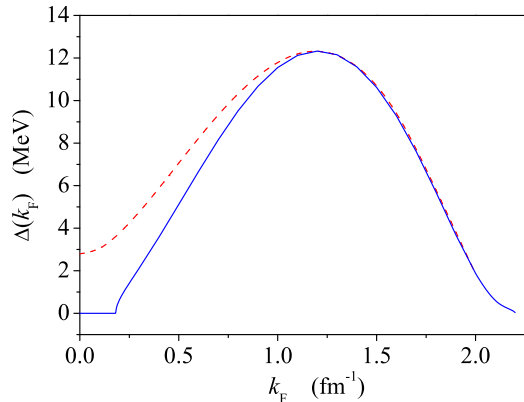


FIG. 6: (Color online) The gap value  $\Delta(k_F)$  found from the solution of the gap equation (dashed curve) and imaginary part of the eigenvalue  $E_b$  for the  ${}^3SD_1$  channel in symmetric nuclear matter.

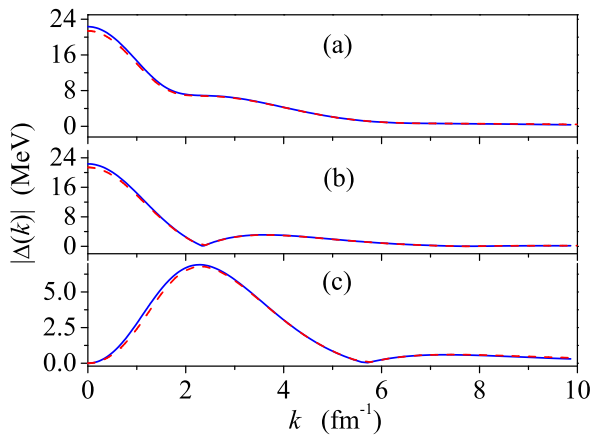


FIG. 7: (Color online) The total pairing gap  $\Delta(k)$  (a) and the partial  $S$  (b) and  $D$  (c) gaps found from the solution of the gap equation (dashed curve) and from the bound state wave function for the  ${}^3SD_1$  channel in symmetric nuclear matter at  $k_F=1.2 \text{ fm}^{-1}$ .

eigenvalue  $E_0$  is significantly below the  $2\varepsilon_F$ . This may indicate that the BCS approximation is not appropriate to describe the strong  $NN$  correlations between protons and neutrons at these densities. This would also explain why one does not observe any features of proton-neutron BCS pairing in finite nuclei.

The Fig. 6 also reflects the fact that at  $k_F$  around  $1.2 \text{ fm}^{-1}$ , which is not far from the saturation density, the results for  $\Delta(k_F)$  coincide. The same is also true for the momentum dependence of the pairing gap  $\Delta(k)$  as can be seen from Fig. 7.

## V. SUMMARY

In the paper we have developed a simple technique which allows to evaluate the function of BCS pairing gap  $\Delta(k)$  in terms of the complex eigenvalue and corresponding eigenfunctions of the  $pphh$  RPA Hamiltonian. With realistic  $NN$  interactions this approach provides results for the gap function in neutron matter which are in a very good agreement with those derived from a conventional solution of the BCS equation.

The study of the bound states of the  $pphh$  RPA Hamiltonian yields results different from the BCS approach if one considers the strong two-nucleon correlations between protons and neutrons indicating a transition from a BEC of quasi-deuterons to the formation of corresponding BCS pairs.

The connection between the BCS approach and the  $pphh$  RPA Hamiltonian established here leads to a generalization of the BCS approach into a treatment of two-particle correlations within the scheme of self-consistent calculations for one- and two-particle Green's function (SCGF).

In this short paper we present results for the approach which treats the single-particle Green's function in the mean-field approximation. However the discussing model contains important features of a general treatment. Thus, the approach can be generalized to a realistic case in a straightforward manner. The corresponding investigations are in preparation.

**Acknowledgments.** The authors appreciate the financial support from the DFG grant MU 705/10-1, the joint DFG-RFBR grant 16-52-12005 and the RFBR grant 16-02-00049.

- 
- [1] A.A. Abrikosov, L.P. Gorkov, I.E. Dzyaloshinski, *Quantum field theoretical methods in statistical physics* (sec. edition, Pergamon press, 1965).
  - [2] J.R. Schrieffer, *Theory of Superconductivity* (Perseus Books, New York, 1999).
  - [3] M. Baldo, J. Cugnon, A. Lejeune, and U. Lombardo, Nucl. Phys. **A515**, 409 (1990).
  - [4] O. Elgaroy, L. Engvik, M. Hjorth-Jensen, and E. Osnes, Nucl. Phys. **A604**, 466 (1996).
  - [5] J. Kuckei, F. Montani, H. Mther, and A. Sedrakian, Nucl. Phys. **A723**, 32 (2003).
  - [6] D. Page, M. Prakash, J.M. Lattimer, and A.W. Steiner, Phys. Rev. Lett. **106**, 081101 (2011).
  - [7] W.C.G. Ho and C.O. Heinke, Nature (London) **462**, 71 (2009).
  - [8] Saras Srinivas, S. Ramanan, Phys. Rev. C **94**, 064303 (2016).
  - [9] T. Alm, G. Röpke, and M. Schmidt, Z. Phys. A **337**, 355 (1990).
  - [10] B.E. Vonderfecht, C.C. Gearhart, W.H. Dickhoff, A.

- Polls, and A. Ramos, Phys. Lett. B **253**, 1 (1991).
- [11] M. Baldo, U. Lombardo, and P. Schuck, Phys. Rev. C **52**, 975 (1995).
- [12] H. Mütter and W.H. Dickhoff. Rev. C **72**, 054313 (2005).
- [13] W. H. Dickhoff and D. Van Neck, *Many-Body Theory Exposed!* (World Scientific, Singapore, 2005).
- [14] R.B. Wiringa, V.G.J. Stoks, and R. Schiavilla, Phys. Rev. C **51**, 38 (1995).
- [15] R. Machleidt, F. Sammarruca, and Y. Song, Phys. Rev. C **53**, R1483 (1996).
- [16] T. Frick, H. Mütter, A. Rios, A. Polls, and A. Ramos, Phys. Rev. C **71**, 014313 (2005).
- [17] H. Mütter, O.A. Rubtsova, V.I. Kukulin, and V.N. Pomerantsev, Phys. Rev. C **94**, 024328 (2016).
- [18] S. Ramanan, S.K. Bogner, R.J. Furnstahl, Nucl. Phys. A **797**, 81 (2007).
- [19] O.A. Rubtsova, V.I. Kukulin, V.N. Pomerantsev and H. Mütter, in preparation.
- [20] M. Matsuo, Phys. Rev. C **73**, 044309 (2006).
- [21] M. Stein, A. Sedrakian, X.-G. Huang, and J.W. Clark, Phys. Rev. C **90**, 065804 (2014).